PRINCE: A Software Tool for Characterizing Waves and Instabilities in Plasma Thrusters

Sebastián Rojas Mata* and Edgar Y. Choueiri†

Electric Propulsion and Plasma Dynamics Lab, Princeton University, Princeton, NJ, 08544, USA

Benjamin Jorns‡

Jet Propulsion Laboratory, California Institute of Technology, Pasadena, CA, 91109, USA

Rostislav Spektor§

The Aerospace Corporation, El Segundo, CA, 90245, USA

An interactive software tool is developed to characterize the waves and instabilities present in plasma thrusters by solving for the complex zeros of plasma dispersion relations. This tool helps researchers explore plasma waves and instabilities in their particular plasma thruster configuration. A user-friendly graphical interface allows versatile data input and parametric control. The zeros of the dispersion relation are located and tracked by root-finding algorithms based on Cauchy's Argument Principle and Newton-Raphson's method. Information about the instabilities found is presented through various data visualization options. The software tool is validated by reproducing previous work concerning instabilities arising in Hall thrusters from solutions to a simplified Esipchuk-Tilinin dispersion relation.

Nomenclature

ω	Angular frequency, rad/s
k	Wavenumber, /m
λ	Wavelength, m
p	Plasma parameter
n	Density, /m^3
T	Temperature, eV
ϕ	Potential, V
B	Magnetic field, G
u	Velocity, m/s
m	Gas mass, kg
λ_D	Debye length, m
v_A	Alfvén velocity, m/s
u_{dey}	$\mathbf{E} \times \mathbf{B}$ electron drift velocity, m/s
u_B	Magnetic drift velocity, m/s

Subscript

e	Electron
i	Ion
o	Neutral
p	Plasma
c	Cyclotron

*Graduate Student, MAE Department, and AIAA Student Member.

†Chief Scientist, EPPDyL, Professor, Applied Physics Group, MAE Department, and AIAA Fellow.

‡Associate Engineer, Electric Propulsion Group, Jet Propulsion Laboratory.

§Laboratory Manager, Propulsion Science.

I. Introduction

Waves and instabilities in a plasma thruster's discharge can affect the theoretical modeling and practical aspects of the device's operation as well as its implementation in spacecrafts. For example, high-frequency radiation emitted by the plume of a plasma thruster can interfere with nearby communications equipment on a spacecraft. Reliable operation of a plasma thruster itself can be compromised by the presence of a plasma wave. This is the case in Hall thrusters, where oscillations in the 1-20 kHz band can have amplitudes on the order of the discharge voltage and sometimes lead to the discharge extinguishing.[1] The effects of plasma waves in Hall thrusters are also part ongoing research involving theoretical modeling of the observed 'anomalous' electron current. Since the applied radial magnetic field in these devices hinders the flow of electrons to the upstream anode, cross-field electron transport models include effects of plasma waves[2–5] to predict the axial electron current. Unfortunately, the models developed so far underestimate the anomalously high measured electron current[6] and have yet to develop a fully self-consistent approach of the physics involved.[7,8]

Determining the dependence of plasma waves and instabilities on operational parameters can guide modeling efforts or help mitigate problems in the thruster's operation. For example, characterizing the linear stability of a wave as a function of controllable magnetic field profiles or mass flow rates informs researchers of desirable parameter spaces at which to operate. Similarly, finding where in the thruster instabilities arise aids focus refined modeling efforts to the regions where the effects of plasma waves are relevant. Plasma waves are analyzed by deriving a dispersion relation of the form $\mathcal{D}(\omega, \mathbf{k}; p_1, p_2, \dots) = 0$ from models of plasma discharges. The complex zeros of $\mathcal{D}$ characterize the wave modes or branches of the dispersion relation that arise in the plasma. Exploring the dependence of these complex zeros on operational parameters across relevant frequency or wavenumber ranges yields valuable information to researchers. However, currently there is no tool available to readily conduct these types of investigations based on input from a particular plasma thruster configuration.

In this paper we present the **P**lasma **R**ocket **In**stability **C**haracteriz**e**r (PRINCE), an interactive software tool which allows researchers to carry out parametric investigations of waves and instabilities for their particular plasma thruster configuration. Based on versatile data input from the user, PRINCE computes plasma dispersion relations and solves for their complex zeros. The goal is to provide the user a robust method to characterize the initially linear oscillations that may arise in a particular plasma thruster. This serves as a first step for approaching plasma thruster instability physics to aid develop analytical or numerical models or guide experimental investigations. We present the features and underlying mathematics of PRINCE along with a representative example of its use as follows. In Section II we describe the program's three main components: the graphical user interface for data input in Section II.A, the implemented root-finding algorithms in Section II.B, and the data visualization capabilities in Section II.C. We validate PRINCE in Section III with a brief characterization of an instability potentially found in Hall thrusters and end with concluding remarks in Section IV.

II. Components of PRINCE

PRINCE has three main components: 1) a graphical user interface, 2) robust root-finding and tracking algorithms, and 3) data visualization routines to provide insight into the numerical results. The current version is implemented in Wolfram Research's Mathematica 10.4 with plans to have future versions be stand-alone programs which run computationally intensive routines in a compiled language such as C++. In the subsections below we describe the features and details of each of these components.

A. Graphical User Interface

The graphical user interface is divided into three panels. In the **Plasma Parameters** panel, shown in Figure 1, the user inputs information concerning various physical parameters of the thruster plasma. PRINCE accepts discrete spatially-resolved data for eight different parameters as a function of zero, one, or two coordinates (Cartesian in the current version). The user specifies the units of the coordinate system and gas species at the bottom of the panel. PRINCE determines the spatial discretization from the imported data and calculates any gradients required by the dispersion relation.

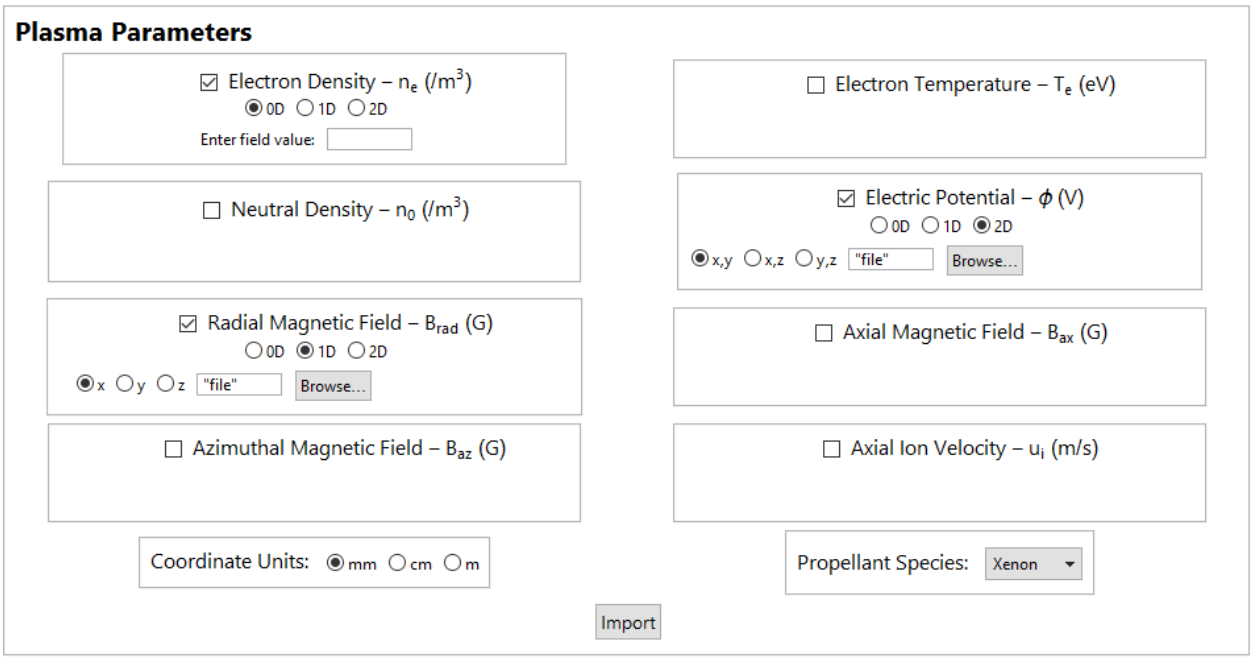

Figure 1. Plasma Parameters Panel. The tool offers several dimensionality and Cartesian coordinate dependence options for eight different input parameters. The user also specifies the units of the input spatial discretization as well as the working gas species.

In the **Solver Settings** panel, shown in Figure 2, the figure at the left displays the orientation of the Cartesian coordinate system as well as dynamically updated vectors of selected electric and magnetic fields. The user chooses from the dropdown menu a pre-set dispersion relation for PRINCE to solve, which displays in the middle of the panel and dynamically updates as the user selects input parameters to include. The present options include a (simplified or full) Esipchuk-Tilinin dispersion relation, warm damped Langmuir waves, and high-frequency $\mathbf{E}\times\mathbf{B}$ drift waves. The required and optional parameters for the selected dispersion relation appear at the right informing the user of the scope of applicable input. Future versions of PRINCE will include more pre-set options as well as allow the user to input a custom dispersion relation through a palette.

At the bottom of the panel the user specifies the dependent variable of the zeros and the range over which to track their locations. Future versions of PRINCE will have an additional panel that displays spatially-resolved calculated plasma characteristic parameters such as cyclotron frequencies that will help the user choose a relevant ω or $\mathbf{k}$ parameter space to explore. Only one of the wavevector components can be iterated over or solved for during one run of the program, so fixed values for the other two components need to be set. For example, the user can choose k_x as the dependent variable and fix k_y and k_z to characterize the waves for varying degree of propagation in the x-direction. PRINCE would then calculate numerical solutions to $\omega(k_x)$ over the range and at the resolution specified for k_x at every spatial point. The user can analyze and output these results with the features of the **Data Visualization** panel described in Section II.C.

B. Algorithms for Root-Solving

We first overview the procedure to numerically solve for the zeros of the dispersion relation before presenting descriptions of the mathematics of the root-finding algorithms. For clarity, we assume the user wants to solve for ω over a range of k_y, implying fixed values for k_x and k_z. However, the user can permute the $\mathbf{k}$ components in this configuration or switch to an iteration over ω and solve for one of the $\mathbf{k}$ components, specifying fixed values for the other two. These options allow the user to characterize waves based on direction of propagation and the range of interest of wavelength or frequency as well as explore the convective or absolute nature of an instability.

PRINCE begins by evaluating the input plasma parameters in the dispersion relation at each spatial point, simplifying $\mathcal{D}(\omega, \mathbf{k}; q_1, q_2 \dots)$ to a set of point-specific $\mathcal{D}(\omega, \mathbf{k})$ functions. Any necessary parameter

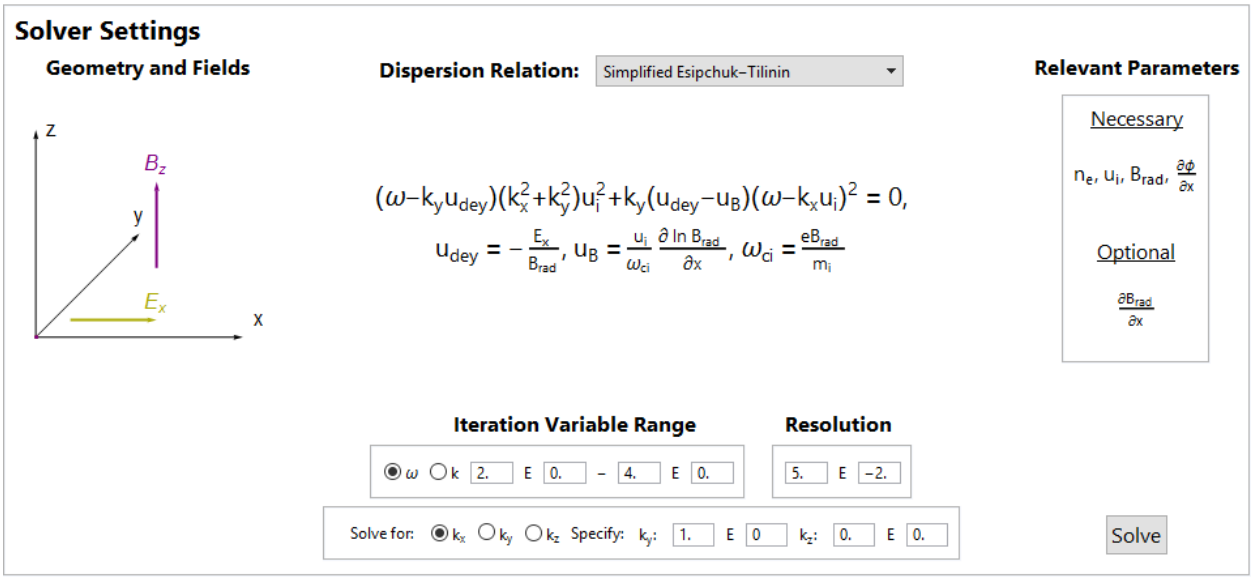

Figure 2. Solver Settings Panel. The dynamically updated figure at left helps the user input the desired magnetic and electric fields. The selected dispersion relation and secondary quantities change as the user picks parameters to include from the list at right. Variable specifications at the bottom serve as input to the iterative root-tracker.

gradients or secondary quantities, such as thermal velocities or cyclotron frequencies, are calculated directly from the imported data or through third order interpolations. To simplify to functions of a single variable $\mathcal{D}(\omega)$, PRINCE evaluates each $\mathcal{D}(\omega, \mathbf{k})$ at the minimum value of k_y, chosen to be the starting point of the root-tracking iteration, and the fixed values of k_x and k_z. A global root-finding algorithm based on Cauchy's Argument Principle[9] and described in Section II.B.1 then finds the initial number of zeros and estimates for their locations in the complex ω-plane for each $\mathcal{D}(\omega)$. PRINCE passes the initial estimates of the zeros' locations to the more efficient local root-finding Newton-Raphson's method to calculate more accurate values. PRINCE uses a different root-finding algorithm at the start of the first iteration step since at that stage no information is available on the location or number of zeros of $\mathcal{D}(\omega)$, which the Newton-Raphson method requires to reliably converge to the correct zero. The iterative procedure described in Section II.B.2 continues using the Newton-Raphson algorithm to track the location of each zero in the complex ω-plane as k_y increments over the user-specified range. The result of the calculations is a set of point-specific numerical solutions for the zeros $\omega(k_y)$ initially located in the physically relevant search region which characterize the oscillation modes for varying degrees of propagation in the y-direction.

1. *Global Root-Finding*

While several algorithms exist to find a zero of a complex function, many involve an iterative procedure that requires an initial guess for the location of the zero.[10] Moreover, which zero (if there are multiple) the iteration converges to can be a highly sensitive or even chaotic function of the initial guess. This presents difficulties when root-finding as it requires the user have some *a priori* knowledge on the number and locations of the zeros of the function for the algorithm to converge to the correct zero. The dispersion relations studied in plasma physics can commonly have an unknown (possibly infinite) number of complex zeros, so this knowledge is not readily determined for an arbitrary non-linear $\mathcal{D}(\omega, \mathbf{k}; q_1, q_2, \dots)$. We therefore design PRINCE to not require such knowledge as input from the user and instead autonomously determine it. To accomplish this, we implement a global root-finding algorithm based on previous work by Choueiri[11,12] that takes advantage of the meromorphic nature of plasma physics dispersion relations.

Consider a meromorphic (analytic except for poles) function $f(z)$ and an analytic function $g(z)$ in a simply-connected open domain $\mathcal{R}$. Assuming that $f(z)$ and $g(z)$ are analytic and $f(z)$ is non-zero on the

positively-oriented closed contour γ bounding $\mathcal{R}$, Cauchy's Argument Principle states that

$$\frac{1}{2\pi i}\oint_{\gamma} g(\zeta)\frac{f'(\zeta)}{f(\zeta)}\,d\zeta = \sum_{k} m_k g(z_k) - \sum_{p} d_p g(z_p), \tag{1}$$

where z_k and z_p are the zeros and poles of $f(z)$ contained in $\mathcal{R}$ with multiplicities m_k and d_p, respectively. Assuming $f(z)$ has no poles in $\mathcal{R}$, thus removing the summation over p above, and letting $g(z) = z^t$, we use Eq. 1 to define the contour integral

$$I_t = \frac{1}{2\pi i}\oint_{\gamma} \zeta^t\,\frac{f'(\zeta)}{f(\zeta)}\,d\zeta = \sum_{k} m_k z_k^t. \tag{2}$$

For the case $t = 0$, the integral gives the sum of the multiplicities of the zeros contained in $\mathcal{R}$. If the domain contains only one zero, then for the case $t = 1$ the integral gives the value of the zero times its multiplicity.

PRINCE conducts the search for the initial zeros of the dispersion relation by substituting each $\mathcal{D}(\omega)$ for $f(z)$ in Eq. 2 and evaluating I_t over a physically relevant search domain $\mathcal{S}$. We can guarantee the $\mathcal{S}$ we consider contains no poles as most $\mathcal{D}(\omega, \mathbf{k}; q_1, q_2, \dots)$ do not have poles or their locations are known from the start,[13,14] justifying the removal of the second summation in Eq. 1. The non-relativistic and quasi-neutrality considerations applicable to plasma thrusters determine the extent of the search domain in the real and imaginary directions. For the search over an ω domain, the upper bound on the zero corresponds to roughly non-relativistic particle motion over a Debye length ($\omega\lambda_D \leq c$). If instead the search were over a $\mathbf{k}$ component domain, the upper bound on the zero is such that the corresponding wavelength is greater than the local Debye length ($k = 2\pi/\lambda \leq 2\pi/\lambda_D$). Additionally, the search excludes strictly real or purely imaginary zeros, which correspond to linearly stable waves or non-propagating oscillations. These zeros can be more computationally intensive to resolve and are less consequential to waves and instabilities studies.

The algorithm to find the number and locations of the initial zeros of the dispersion relation is as follows:[11]

1. Divide the search domain $\mathcal{S}$ in the complex ω-plane into rectangular cells.
2. For each cell, evaluate I_0 numerically along the delimiting contour.
3. For each cell, take one of three actions based on the value of I_0:
   (a) If $\Re\{I_0\} = 1$ within tolerance, a simple zero was found, so calculate and store I_1 as the estimate for its location.
   (b) If $\Re\{I_0\} = 0$ within tolerance, no zeros are contained in the cell, so disregard it.
   (c) If $|\Re\{I_0\}| > 0$ and $|1 - \Re\{I_0\}| > 0$ within tolerance, the cell may contain unresolved zeros, so label the cell as suspect.
4. If there are no suspect cells, all zeros were found and the search terminates. Otherwise, for each suspect cell there are two options:
   (a) If $\mathcal{D}\left(I_1/\Re\{I_0\}\right) = 0$ within tolerance, the cell contains a single degenerate zero with multiplicity $\Re\{I_0\}$, so store $I_1/\Re\{I_0\}$ as the estimate for its location.
   (b) If $\mathcal{D}\left(I_1/\Re\{I_0\}\right) \neq 0$ within tolerance, the suspect cell contains unresolved zeros, so recursively apply the algorithm to the cell.

Figure 3 illustrates this procedure for the example of four zeros, three of which correspond to physically relevant, linearly unstable waves. The sign of the real part of the zero indicates whether the wave's phase velocity is parallel or anti-parallel to the (k_x, k_y, k_z) vector. The search domain $\mathcal{S}$ is the union of four disjoint rectangular regions, one in each quadrant of the complex plane and each off-set from the real and imaginary axes by a predefined distance. PRINCE recursively applies the search algorithm only to the suspect cells containing unresolved zeros (Cell B in this example). The other cells are discarded once the number and locations of any resolved zeros are stored.

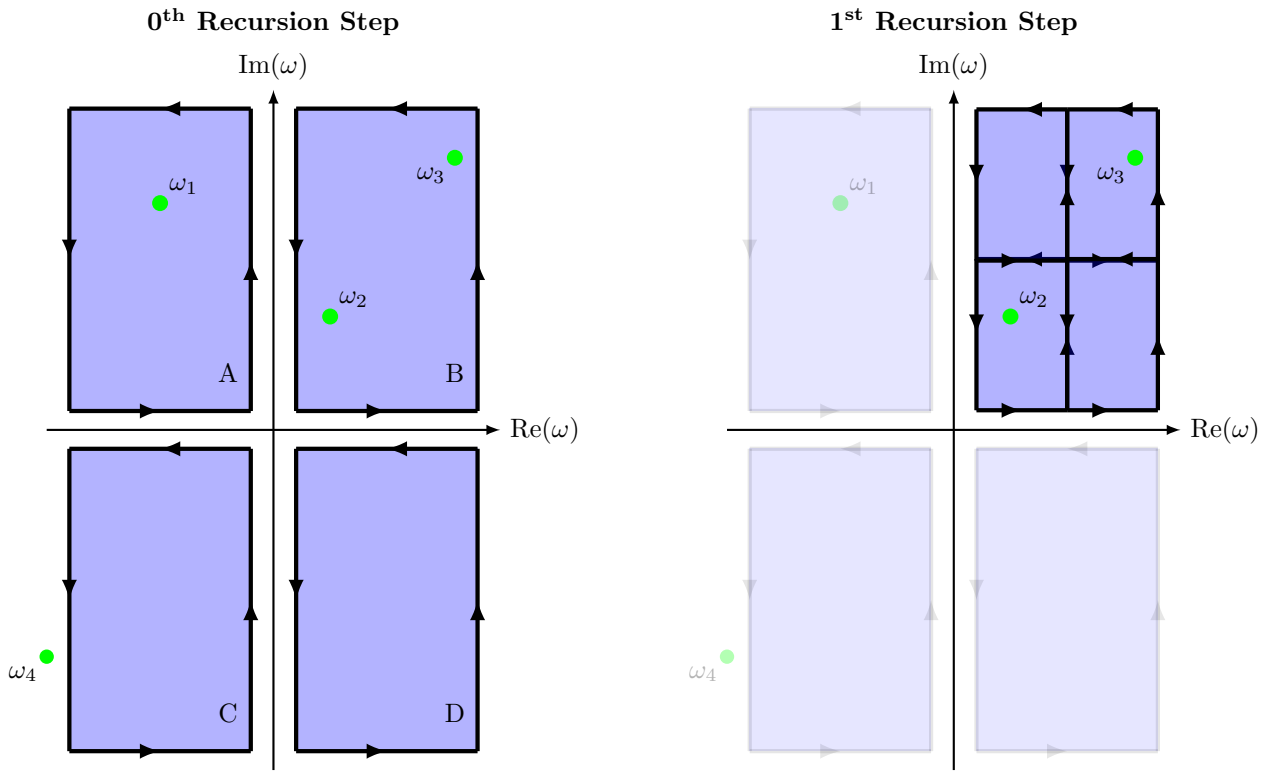

Figure 3. Root-Finding Recursion. The tool determines in the 0th Recursion Step that cells C and D contain no zeros while cell A only contains zero ω_1. Cell B is suspect, so it is subdivided into smaller cells in the 1st Recursion Step to resolve zeros ω_2 and ω_3. As zero ω_4 is not inside any of the search cells, it is ignored.

2. Iterative Local Root-Tracking

Once the global root-finding algorithm finds and calculates the initial locations of the physically relevant zeros of each $\mathcal{D}(\omega)$, PRINCE passes this information to an iterative local root-tracking routine. Now that knowledge regarding the zeros is available, we implement Newton-Raphson's method, which requires adequate initial guesses as input, to track these zeros as k_y increments over the user-specified range. At the first iteration step, PRINCE refines the initial locations of the zeros using the values calculated with I_1 as initial guesses for the Newton-Raphson solver. In the following iteration steps, PRINCE re-evaluates the dispersion relation at the new value of k_y and uses the zeros' locations from the previous step as initial guesses for the Newton-Raphson algorithm to determine the new locations of the zeros. The process continues until PRINCE completes the iteration over the specified k_y range.

C. Data Visualization

PRINCE provides data visualization routines to interpret the results of the numerical solver. Raw data output is also available if the user wishes to conduct their own analysis on the numerical results. The data visualization features currently available in PRINCE highlight the relevant information of the zeros with the largest positive imaginary part (growth rate) across all branches at a spatial point, i.e. the most unstable mode which will dominate due to its exponential growth.

From the **Data Visualization** panel the user can output the real and imaginary parts of the zeros as a function of the iteration variable for each branch at each spatial point. The **Single Branch** button plots the value of the zero as a function of the iteration variable for an individual branch at a spatial point; this is the only local data visualization feature. The **Binary Instability Spatializer** option shows for each spatial point the binary status (yes or no) of an instability's prescence. This serves to readily visualize the regions where instabilities arise. Two contour plots available under the **Dominant Unstable Mode** section display information related to the zero with the largest growth rate across all branches at each spatial point. The plots show either the value of the iteration variable at which the zero attains that growth rate or the

real part of the zero that accompanies that growth rate.

III. Validation

We validate PRINCE by reproducing previous work[1] which investigated instabilities arising in a Hall thruster channel from solutions to the Esipchuk-Tilinin dispersion relation[15]

$$\frac{1}{\omega_{\rm pi}^2} - \frac{1}{(\omega - k_x u_{\rm i})^2} + \frac{1}{\omega_{\rm ce}\omega_{\rm ci}} + \frac{1}{k_\perp^2 v_A^2} - \frac{k_y(u_{dey} - u_B)}{k_\perp^2 u_{\rm i}^2(\omega - k_y u_{dey})} = 0. \tag{3}$$

Here $\omega_{\rm pi}$ is the ion plasma frequency, $u_{\rm i}$ the ion velocity, $\omega_{\rm ce}$ and $\omega_{\rm ci}$ the electron and ion cyclotron frequencies, v_A the Alfvén velocity, u_{dey} the $\mathbf{E}\times\mathbf{B}$ electron drift velocity, and u_B the magnetic drift velocity. Ref. 1 restricted the frequency range considered such that $(\omega - k_x u_i)^2 \ll \omega_{\rm ce}\omega_{\rm ci} \ll \omega_{\rm pi}^2$ and $(\omega - k_x u_i)^2 \ll k_\perp^2 v_A^2$ to simplify the dispersion relation to

$$\frac{1}{(\omega - k_x u_{\rm i})^2} + \frac{k_y(u_{dey} - u_B)}{k_\perp^2 u_{\rm i}^2(\omega - k_y u_{dey})} = 0, \tag{4}$$

so this is the version we analyze with PRINCE. Extracted experimental data sets with xenon as propellant[16] with a spatial resolution of 0.5 mm of electron density, electric potential, and radial magnetic field, reproduced in Figure 4(a)-(c), served as input to calculate $u_{\rm i}$, $u_{dey} = -E_y/B_{\rm rad}$, $\omega_{\rm ci} = eB_{\rm rad}/m_{\rm i}$, and $u_B = \frac{\partial B_{\rm rad}}{\partial x} u_{\rm i}/\omega_{\rm ci}$ in both the previous work and our reproduction.

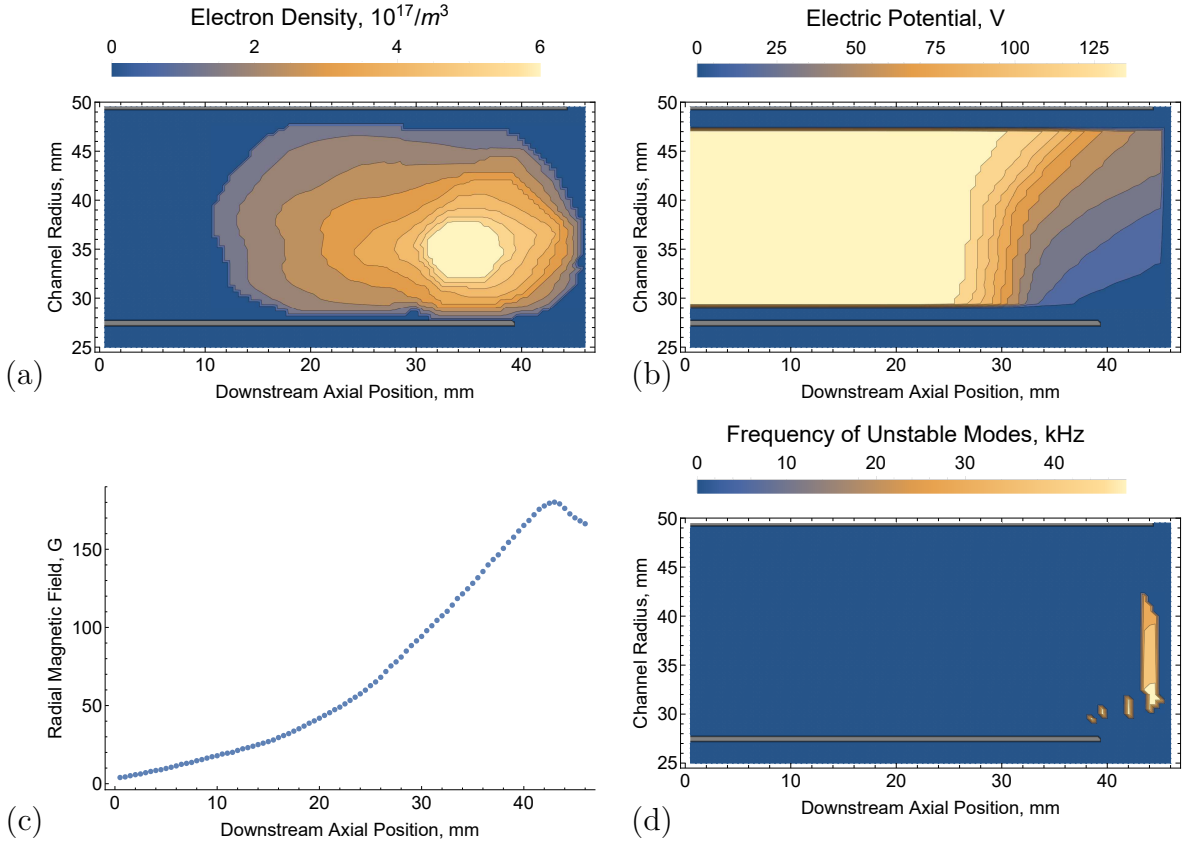

Figure 4. Esipchuk-Tilinin Dispersion Relation Example. Profiles of the electron density, electric potential, and radial magnetic field extracted from Ref. 16 display in panels (a), (b), and (c), respectively. The real frequency of the unstable modes of Eq. 4 with $k_\perp = 1/z$ and mostly azimuthal propagation ($k_y = 10k_x$) are displayed in panel (d). Blue denotes stable regions.

Ref. 1 characterized instabilities arising in the mostly azimuthal propagation ($k_y = 10k_x$) of the mode with $k_\perp = \sqrt{k_x^2 + k_y^2} = 1/z$, where z is the local radius of curvature of the channel. The results comprise

computations of the complex zeros $\omega(k_x, k_y)$ using the analytical solution of Eq. 4. Figure 9(f) in Ref. 1 plots the real part of the zeros at the locations where the zero has a positive imaginary part, signifying the mode is unstable. To reproduce this analysis, we use PRINCE to characterize the zeros $\omega(\mathbf{k})$ of Eq. 4. We set $k_z = 0$ and $k_y = 10k_x$ and vary k_x between 2 m^{-1} and 4 m^{-1} at a resolution of 0.05 m^{-1}. We extract the value of ω corresponding to the mode $k_\perp = 1/z$ for each spatial point from the output raw data to produce Figure 4(d), our reproduction of Figure 9(f) from Ref. 1. The locations where instabilities arise match well, corresponding as expected to the region in the channel where the radial magnetic field gradient is negative with respect to the axial variable ($\partial B_{\text{rad}}/\partial x < 0$). The frequency range (20-50 kHz) is also comparable, differences no larger than 10 kHz potentially due to different interpolation schemes used to calculate the gradients and secondary plasma quantities.

IV. Conclusion

We presented the interactive software tool PRINCE which aids users characterize plasma waves by finding and tracking the zeros of dispersion relations. Researchers can use PRINCE to conduct exploratory investigations of plasma instabilities arising in their particular plasma thruster configuration. Using versatile data input from the user, PRINCE implements a global root-finding algorithm to search for the locations of the complex zeros of dispersion relations. An iterative procedure then uses a local root-finding algorithm to track the zeros over a user-specified range, resulting in numerical solutions of the zeros which characterize the wave modes that can arise in the plasma thruster. We validate PRINCE by reproducing the results of previous work concerning instabilities arising from a simplified version of the Esipchuk-Tilinin dispersion relation in the channel of a Hall thruster. Future versions of the program will feature more intricate and customizable dispersion relations and solver settings as well as advanced data post-processing and visualization features.

Acknowledgements

A portion of the research was carried out at the Jet Propulsion Laboratory, California Institute of Technology, under a contract with the National Aeronautics and Space Administration.

References

[1]Choueiri, E. Y., "Plasma Oscillations in Hall Thrusters," *Physics of Plasmas*, Vol. 8, No. 4, 2001, pp. 1411–1426.

[2]Heron, A. and Adam, J. C., "Anomalous conductivity in Hall thrusters: Effects of the non-linear coupling of the electron-cyclotron drift instability with secondary electron emission of the walls," *Physics of Plasmas*, Vol. 20, No. 8, 2013, pp. 82313.

[3]Yoshikawa, S. and Rose, D. J., "Anomalous Diffusion of a Plasma across a Magnetic Field," *Physics of Fluids*, Vol. 5, No. May 2015, 1962, pp. 334.

[4]Cappelli, M. A., Meezan, N. B., and Gascon, N., "Transport physics in Hall plasma thrusters," *40th AIAA Aerospace Sciences Meeting and Exhibit*, Reno, NV, 2002.

[5]Adam, J. C., Boeuf, J. P., Dubuit, N., Dudeck, M., Garrigues, L., Gresillon, D., Herón, A., Hagelaar, G. J. M., Kulaev, V., Lemoine, N., Mazouffre, S., Perez Luna, J., Pisarev, V., and Tsikata, S., "Physics, simulation and diagnostics of Hall effect thrusters," *Plasma Physics and Controlled Fusion*, Vol. 50, No. 12, 2008, pp. 124041.

[6]Janes, G. S. and Lowder, R. S., "Anomalous Electron Diffusion and Ion Acceleration in a Low-Density Plasma," *The Physics of Fluids*, Vol. 9, No. 6, 1966.

[7]Spektor, R., "Quasi-Linear Analysis Of Anomalous Electron Mobility Inside A Hall Thruster," *30th International Electric Propulsion Conference*, Florence, Italy, 2007, pp. 1–10.

[8]Litvak, A. A. and Fisch, N. J., "Resistive Instabilities in Hall Current Plasma Discharge," *Physics of Plasmas*, Vol. 8, No. 2, 2001, pp. 648–651.

[9]Brown, J. W. and Churchill, R. V., *Complex Variables and Applications*, McGraw Hill, New York, 8th ed., 2009.

[10]Kowalczyk, P., "Complex Root Finding Algorithm Based on Delaunay Triangulation," *ACM Transactions on Mathematical Software*, Vol. 41, No. 3, 2015.

[11]Choueiri, E. Y., *Electron-Ion Streaming Instabilities of an Electromagnetically Accelerated Plasma*, Phd, Princeton University, 1991.

[12]EPPDyL, *DART Tool: Dispersion relation solver*, 2012.

[13]Martin, T. J., "Root finding and the solution of dispersion equations," Tech. Rep. CLM-PDN-3/71, Culham Laboratory, Abingdon Berkshire, UK, 1971.

[14]Stix, T. H., *Waves in Plasma*, Springer-Verlag, New York, 1st ed., 1992.

[15]Esipchuk, Y. B. and Tilinin, G. N., "Drift instability in a Hall-current plasma accelerator," *Sov. Phys. Tech. Phys.*, Vol. 21, No. 4, 1976, pp. 417–423.

[16]Bishaev, A. M. and Kim, V., "Local plasma properties in a Hall-current accelerator with an extended acceleration zone," *Soviet Physics, Technical Physics*, Vol. 23, No. 9, 1978, pp. 1055–1057.